DOI: 10.1002/chem.200701927

# Theoretical Investigation of Clusters of Phosphorus and Arsenic: Fascination and Temptation of High Symmetries

**Paola Nava and Reinhart Ahlrichs*[a]**

**Abstract:** We present a theoretical study of the energetic and thermodynamic stability of selected phosphorus and arsenic clusters containing 18 to 168 atoms. For this purpose we employ MP2 as well as DFT functionals BP86 and B3LYP with extended basis sets. All procedures predict the family of one-dimensional polymers $X_{18+12n}$, each with $2^{n-1}$ isomers of virtually identical energy, to be more stable than other structures investigated so far. Furthermore, islands of stability result for ring-shaped clusters $X_{24n}$ with $D_{nd}$ symmetry for $n=4$ (only for arsenic), 5, 6, and 7. Phosphorus and arsenic show otherwise a very similar behavior. An investigation of basis set effects shows that a doubly polarized triple zeta valence basis (TZVPP) is both necessary and sufficient. In comparison to the reliable spin component scaled MP2 (SCS-MP2) procedure, DFT methods underestimate and MP2 overestimates the stability of larger clusters; the discrepancy increases with the number of atoms. The addition of a long-range dispersion correction to B3LYP energies does not rectify the shortcomings of DFT in comparison with SCS-MP2.

**Keywords:** ab initio calculations · arsenic · main group chemistry · phosphorus · structure optimization

## Introduction

Highly symmetric molecules, such as the famous icosahedral species $[B_{12}H_{12}]^{2-}$, $[Al_{12}H_{12}]^{2-}$, and the fullerene $C_{60}$, are fascinating to many chemists.[17,21,39] The aesthetic appeal has motivated the search for further icosahedral clusters or cluster ions, very often led by quantum-chemical investigations. Notable successes in this respect, when predictions were confirmed by experiment, include the impressive recent example $WAu_{12}$.[23,29]

Theoreticians have another reason, besides aesthetics, to consider highly symmetric molecules: the relatively low computational requirements. If $|G|$ denotes the order of the molecular symmetry group G, then CPU times scale as $|G|^{-1}$ to $|G|^{-2}$, provided symmetry exploitation is properly implemented. Integral evaluation (including quadrature) in HF, DFT, and MP2, the only ab initio methods routinely applicable to larger molecules, scales as $|G|^{-1}$,[6] diagonalizations roughly as $|G|^{-2}$, as is obvious from Roothaan's analysis of the treatment of symmetry.[30] The reduction for single-point energy and gradient calculations is enhanced in a geometry optimization due to the smaller number of degrees of freedom, giving roughly an additional $|G|^{-1}$ scaling. Symmetry exploitation thus makes truly impressive quantum-chemical treatments possible.

Karttunen et al.[19,20] have recently applied theoretical methods for $I_h$-symmetric clusters as large as $As_{500}$ and $P_{720}$, and ring-shaped clusters $X_{10n}$ (X=P, As) with symmetry $D_{nh}$ up to $X_{360}$. Dodecahedral $P_{20}$ was long ago computed to be unstable with respect to tetrahedral $P_4$,[12] more recent work reaches the same conclusion for fullerene-like clusters $P_m$, for $m$ between 14 and 60.[9] Karttunen et al. report larger $I_h$-symmetric clusters from $P_{80}$ up to $P_{720}$ to be stable with respect to $P_4$. For As, even $As_{20}$ is found to be lower in energy than five $As_4$. The largest cohesive energies are reported for the ring-shaped clusters $X_{10n}$, which reach a stability maximum around $X_{180}$.

The computed stability of ring-shaped structures poses some questions. The first one concerns the reliability of computational procedures employed by Karttunen et al., B3LYP and MP2, which have known shortcomings. The second concerns the basis sets used: to treat all clusters on the same footing, relatively small basis sets had to be chosen, which may also affect results. Finally, a large variety of low-energy structural motifs is known for clusters of phosphorus from the work of Häser et al.,[4,10,12] and there may be other isomers, which are energetically and thermo-

[a] Dr. P. Nava, Prof. Dr. R. Ahlrichs
Lehrstuhl für Theoretische Chemie
Institut für Physikalische Chemie, Universität Karlsruhe (TH)
Kaiserstrasse 12, 76128 Karlsruhe (Germany)
Fax: (+49) 721-608-7225
E-mail: reinhart.ahlrichs@chemie.uni-karlsruhe.de

  

dynamically favored over the ring-shaped structures. These topics will be addressed in the present work.

## Computational procedures

We performed DFT calculations with functionals BP86[2,25,26,35] and B3LYP,[3,22,32,35] as well as MP2 calculations as implemented in TURBOMOLE.[1,11,33] In MP2 treatments we kept core orbitals frozen: a Ne core for P and an Ar core for As. Preliminary structure optimizations were carried out with BP86 using the small SVP (split valence plus polarization) basis set,[37] followed by analytical force field calculations to compute (harmonic) vibrational frequencies, to establish local minimum character, and to estimate corresponding contributions to the free energy. Final results were obtained with the larger def2-TZVPP basis set[37] (here denoted TZVPP, triple zeta double polarization) for BP86 and B3LYP, and single-point MP2 calculations at the B3LYP geometry. Structure optimizations were done on the basis of redundant internal coordinates.[34] The RI technique (resolution of the identity) was employed in DFT-BP86 and MP2 treatments with appropriate auxiliary basis sets.[14,36] The more CPU-demanding calculations for clusters with over 50 atoms were done with parallel implementations for SCF,[5] B3LYP,[33] and RI-MP2 (module RICC2)[15] on typically eight processors. A genetic algorithm[31] was employed to find low-energy structures for $P_{20}$ and $As_{20}$. The population size was 40, the number of children 32. The search was done with BP86/SVP, the structures located were then refined with the TZVPP basis in BP86 and B3LYP, followed by single-point MP2 calculations. The choice of methods was motivated by the following considerations.

B3LYP and MP2 are proven procedures for the treatment of closed-shell cases with clear-cut single-reference character as considered in this work. B3LYP, as with all DFT functionals, does not account reliably for long-range dispersion interactions,[18,38] and thus tends to underestimate the stability of larger molecules in comparison to smaller ones. MP2, on the other hand, includes dispersion interactions in an approximate way, but it shows a tendency to overestimate these effects.[7,18] This deficiency is rectified to a large extent by the "spin component scaled" procedure (SCS-MP2) of Grimme,[7] which has been shown to be surprisingly accurate, in many cases even close to QCISD(T) and CCSD(T) results.[7,16] It is thus to be expected that SCS-MP2 is more accurate than either B3LYP or MP2. Non-hybrid functionals are typically less accurate for energetics than hybrid functionals. Since we are dealing with relatively simple systems and since BP86 is about an order of magnitude (or more) less demanding computationally than B3LYP, we found it worthwhile to also document BP86 results.

The TZVPP basis was selected since it gives results close to the basis set limit for SCF and DFT treatments, as shown in an extensive benchmark study.[37] TZVPP is also the smallest basis set to yield reasonable reaction energies in correlated treatments. Although basis set convergence is here clearly slower than for SCF or DFT, it may be safely expected that TZVPP is close to the basis set limit for the reactions considered in this work.[37] We checked this assumption in SCS-MP2 treatments of selected smaller clusters by employing a polarized quadruple zeta valence (QZVPP) basis.[37]

In the choice of structures we rely heavily on the comprehensive theoretical studies by Häser et al.[4,10,12,13] We found it worthwhile to check these by an unbiased systematic search for low-energy isomers. This was accomplished by applying a genetic algorithm. $P_{20}$ and $As_{20}$ are just small enough for such a procedure to be feasible; they are also large enough to test Häser's structural rules and the usefulness of the genetic algorithm.

## Structures Considered

The first series considered consists of one-dimensional polymers $X_{18+10n}$, which are depicted for $P_{28}$ and $P_{78}$ in Figure 1. The great stability of these curved $C_{2v}$-symmetric structures was discovered by Häser, and they were also treated by Karttunen et al. for $P_{18}$ up to $P_{78}$.[19] By carrying out a ring closure[19,20] one gets $X_{10n}$ with $D_{nh}$ symmetry (Figure 1). These rings are without strain around $X_{180}$, as can be inferred from corresponding angles of the curved $C_{2v}$ chains, whereas some strain is inevitable below and above that size. This probably causes $X_{80}$ to have the lower symmetry $D_{4d}$ instead of $D_{8h}$; Karttunen et al. found $C_{4v}$, they may have over-

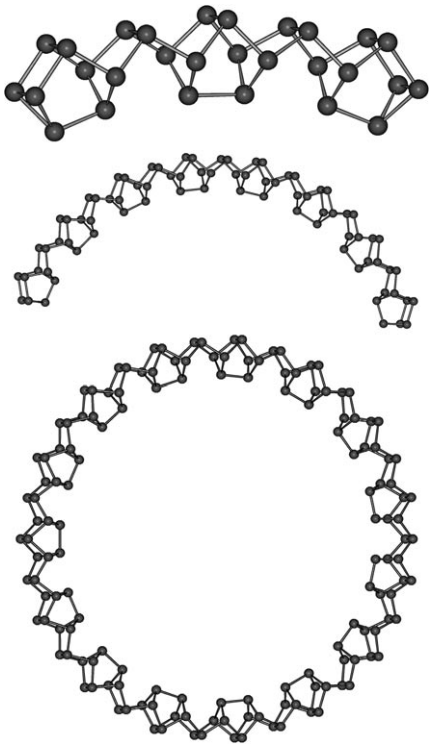

Figure 1. Computed structures of $X_n$ based on the building block ($X_8X_2$), top to bottom: $X_{28}$, $C_{2v}$; $X_{78}$, $C_{2v}$; and $X_{150}$, $D_{15h}$.

  

looked the higher symmetry.[19] The favorable energy of these and other rings results from the absence of $X_8$ end groups, which are relatively high in energy.

A second series of polymers is based on Häser's R-$(P_2P_{10})_nP_2R$ compounds,[4] with end groups $R=P_8$ (Figure 2). (The first members of this and of the preceding series, $X_{18}$, are actually identical.) This structural type leads to a helical geometry (among others, vide infra), and Häser's prediction of pronounced stability was confirmed by the preparation of helical $(P_2P_{10})_\infty$ embedded in a CuI matrix.[27]The chains $(P_2P_{10})_nP_2$ in fact constitute an entire family. In each $(P_2P_{10}P_2)$ unit, the two $P_2$ axes have a torsion angle of roughly 120°, which turns into −120° in the mirror image of this moiety. There is even a third possibility with an eclipsed position of the five-rings, but this is higher in energy by about 55 kJmol$^{-1}$. In building a polymer chain $(P_2P_{10})_nP_2$, one thus has two choices for each $(P_2P_{10}P_2)$ link, which yields $2^{n-1}$ isomers, since the $2^n$ cases come in pairs of mirror images. In Figure 2 we show for $X_{66}$, that is, $n=4$, the two extreme cases: the curved $C_s$ structure with alternating and the helical $C_2$ structure with identical torsional angles. Since all $2^{n-1}$ isomers have identical topology within each $(P_2P_{10}P_2)$ moiety, they are expected to be very close in energy. The curved structures can also be closed to a ring by removing the $P_8$ end groups, as shown in Figure 2 for $X_{120}$. The construction of small ring-shaped clusters requires a large curvature, which can only be achieved by alternating torsion angles within $(X_2X_{10})_2$. This leads to the composition $X_{24n}$ with $D_{nd}$ symmetry. Larger rings can of course also be obtained from chains with a proper choice of torsion angles.

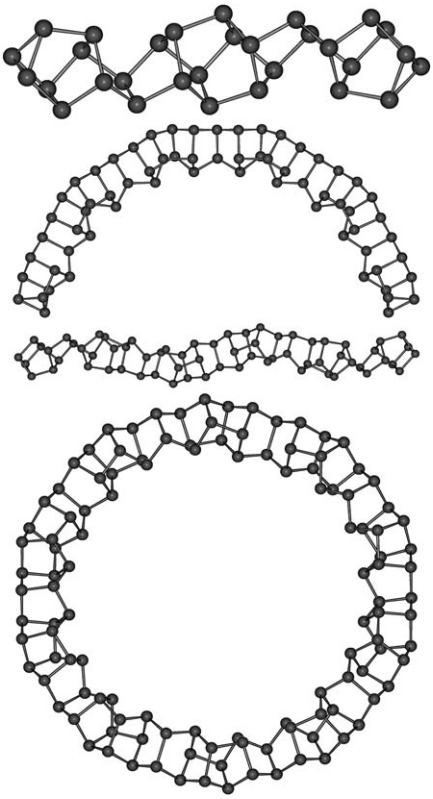

Figure 2. Computed structures of $X_n$ based on the building block $(X_{10}X_2)$, top to bottom: $X_{30}$, $C_2$; curved $X_{66}$, $C_s$; helical $X_{66}$, $C_2$; and $X_{120}$, $D_{5d}$.

$I_h$-symmetric structures were first studied by Häser at al. for $P_{20}$,[12] an extended treatment of larger clusters has recently been carried out by Karttunen et al.,[19] and herein we treat $X_{20}$ and $X_{80}$ for X=P, As (Figure 3). We have furthermore considered other structures proposed by Häser et al.[4] but these turned out to be higher in energy than those of the first two series.[1] In Figure 4 we present the

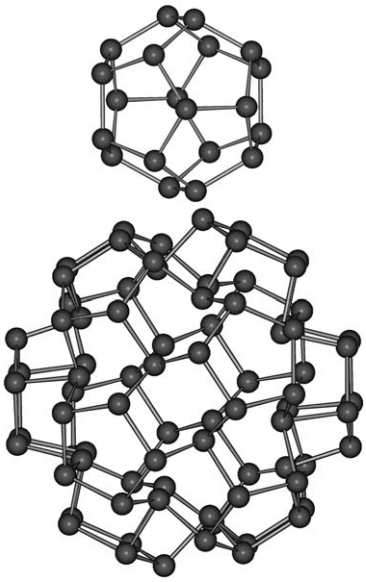

Figure 3. Computed structure of icosahedral $P_{20}$ and $P_{80}$.

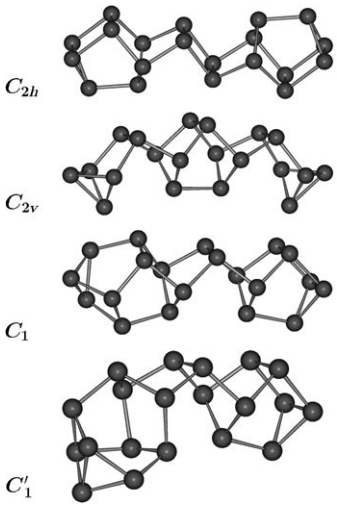


Figure 4. Computed structures of low-lying energy isomers of $X_{20}$.

[1] Those structures included, for example, $P_{58}$, Figure 10d in reference [4], which is the model compound for Hittorf's phosphorus.

  

structures considered for $X_{20}$, which were partly obtained by the genetic algorithm.

For $As_m$ we consider the same structures as for $P_m$. The great similarity of $P_m$ and $As_m$ is,[28] not unexpectedly, shown by the fact that very good starting geometries for a structure optimization can be obtained by simply scaling cartesian coordinates with the ratio of covalence radii, that is, 1.21:1.10. This is also demonstrated by the results of the genetic algorithm: starting from the (scaled) structures of $As_m$ for $P_m$ (or vice versa) did not produce new structural types of low energy and resulted in the same lowest isomers. The similarity of $P_m$ and $As_m$ greatly facilitates structure optimizations by starting with $P_m$, less demanding, and then refining the scaled structures for $As_m$.

## Discussion

Our calculations are limited to clusters with up to 168 atoms, mainly because of computational demands resulting from low molecular symmetries in connection with employing an extended basis set. To give the reader an impression of the computational demands, we report timings for the most expensive calculations. The RI-MP2 energy calculations for $As_{144}$ ($As_{90}$) in $D_{6d}$ ($C_2$) symmetry with 6912 (4320) contractions, 22896 (14310) auxiliaries, and 1080 (675) correlated MOs, required 85 h (78 h) on 12 AMD Opteron 2.5 GHz processors. SCF or B3LYP calculations required in these cases just a few percent of these timings.

Results are discussed on the basis of computed reaction energies relative to those of tetrahedral $X_4$:

$$\Delta E(X_m) = \frac{4}{m} E(X_m) - E(X_4, T_d) \quad (1)$$

Tables 1 and 2 contain $\Delta E(X_m)$ data for X = P and As, and graphical representations of $\Delta E$ for these cases are shown in Figures 5 and 6, respectively.

Table 1. Computed $\Delta E$ data in kJ mol$^{-1}$ ($P_4$) of $P_m$ relative to $P_4$, according to Equation (1), at different levels of theory (def2-TZVPP basis set). G denotes the symmetry group, $\Delta F$ is the computed Helmholtz free energy contribution at ambient conditions, see text for details.

| $m$ | G | BP86 | B3LYP | SCS-MP2 | SCS-MP2 + $\Delta F$ |
|---|---|---|---|---|---|
| genetic algorithm, Figure 4 | | | | | |
| 20 | $C_{2h}$ | −33.1 | −21.8 | −38.7 | 4.5 |
| 20 | $C_{2v}$ | −32.1 | −21.1 | −39.4 | 3.2 |
| 20 | $C_1$ | −31.3 | −19.1 | −36.3 | 6.5 |
| $P_{18+10n}$ $C_{2v}$, Figure 1 | | | | | |
| 18 | $C_{2v}$ | −35.5 | −24.2 | −41.2 | −2.2 |
| 28 | $C_{2v}$ | −42.7 | −30.2 | −52.1 | −5.1 |
| 38 | $C_{2v}$ | −46.1 | −33.0 | −57.1 | −7.9 |
| 58 | $C_{2v}$ | −49.6 | −35.8 | −62.0 | −10.6 |
| 78 | $C_{2v}$ | −51.1 | −37.1 | −64.4 | −12.1 |
| 118 | $C_{2v}$ | −52.7 | −38.4 | −66.8 | – |
| 148 | $C_{2v}$ | −53.3 | −38.9 | – | – |
| ring-shaped $P_{10n}$, Figure 1 | | | | | |
| 80 | $D_{4d}$ | −35.8 | −16.9 | −51.1 | 2.3 |
| 120 | $D_{12h}$ | −52.5 | −36.3 | −68.5 (−85.0)[a] | −13.7 |
| 150 | $D_{15h}$ | −55.0 | −39.5 | −71.0 | – |
| 160 | $D_{16h}$ | −55.3 | −40.0 | – | – |
| $P_{18+12n}$, Figure 2 | | | | | |
| 30 | $C_2$ | −44.2 | −31.4 | −54.3 | −6.6 |
| 42 | $C_2$ | −48.1 | −34.6 | −59.8 | −9.9 |
| 66 | $C_s$ | −51.4 | −37.3 | −64.7 | −12.6 |
| 66 | $C_2$ | −51.5 | −37.4 | −64.9 | −12.8 |
| 78 | $C_2$ | −52.3 | −38.1 | −66.1 | −13.4 |
| 90 | $C_2$ | −53.0 | −38.5 | −67.3 | −13.8 |
| 114 | $C_s$ | −53.8 | −39.3 | −68.4 | −14.9 |
| 138 | $C_s$ | −54.3 | −39.7 | −69.5[b] | – |
| ∞[b] | – | −57.4 | −42.2 | −73.7 | – |
| ring-shaped $P_{24n}$ $D_{nd}$, Figure 2 | | | | | |
| 96 | $D_{4d}$ | −51.1 | −35.1 | −67.0 | −12.3 |
| 120 | $D_{5d}$ | −56.3 | −41.0 | −72.5 | −17.3 |
| 144 | $D_{6d}$ | −57.1 | −42.0 | −73.0 | – |
| 168 | $D_{7d}$ | −56.3 | −41.3 | – | – |
| icosahedral clusters, Figure 3 | | | | | |
| 20 | $I_h$ | 25.3 | 36.6 | 40.8 | 84.0 |
| 80 | $I_h$ | −7.4 | 17.3 | −25.8 | 28.1 |

[a] MP2 value. [b] Extrapolated value for the series $P_{18+12n}$, according to Equation (2).

**Aspects of methodology:** The large spread of B3LYP and SCS-MP2 results is the most striking feature of the computed reaction energies. The corresponding deviations are even larger if one compares the B3LYP results with those from MP2 calculations, as shown for the results obtained for $P_{120}$ and $As_{120}$ with $D_{12h}$ symmetry (Tables 1 and 2). Compared to the SCS-MP2 method, MP2 overestimates the stability of $P_{120}$ by 16.5 kJ mol$^{-1}$ ($P_4$) and that of $As_{120}$ by 18.8 kJ mol$^{-1}$ ($As_4$); a correspondingly smaller (larger) effect is found for the smaller (larger) clusters. We consider this an artefact of MP2, which predicts large clusters to be much too stable.

The considerable spread between $\Delta E_{B3LYP}$ and $\Delta E_{SCS\text{-}MP2}$ results is attributable to the fact that DFT does not properly account for long-range dispersion forces. Following the suggestion by one of the referees, we have also investigated the semiempirical long-range dispersion correction proposed by Grimme[8] on top of B3LYP energies: the B3LYP-D procedure. Single-point B3LYP-D/TZVPP energies have been computed for B3LYP/TZVPP structures, which allow a direct comparison with SCS-MP2 energies collected in Tables 1 and 2. A very consistent trend emerges for clusters with 18 to 66 atoms: B3LYP-D overestimates the stability of $P_n$ by (14 ± 1) kJ mol$^{-1}$ ($P_4$) and that of $As_n$ by (27 ± 1) kJ mol$^{-1}$ ($As_4$) relative to the energies calculated by SCS-MP2. For the small clusters $X_{18}$, this means that B3LYP-D has the same error as B3LYP itself (relative to SCS-MP2), only the sign is reversed. B3LYP-D is clearly not a useful approximation to SCS-MP2 energies for clusters of P and As. Since we are dealing with relatively simple reactions, which involve only closed-shell cases of clear-cut single reference electronic structures, our findings should be taken as one more warning not to overestimate the accuracy of computational procedures, which are only proven for benchmark sets of small molecules.

BP86 is typically inferior to SCS-MP2 and B3LYP for reaction energies. For the cases considered here, it is closer to SCS-MP2 than B3LYP, and a useful guide for relative stabilities. As long as a reliable calibration of computational pro-

  

Table 2. Computed $\Delta E$ data in kJ mol$^{-1}$ ($As_4$) of $As_m$ relative to $As_4$, according to Equation (1), at different levels of theory (def2-TZVPP basis set). G denotes the symmetry group, $\Delta F$ is the computed Helmholtz free energy contribution at ambient conditions, see text for details.

| $m$ | G | BP86 | B3LYP | SCS-MP2 | SCS-MP2+$\Delta F$ |
|---|---|---|---|---|---|
| genetic algorithm, Figure 4 | | | | | |
| 20 | $C_{2h}$ | −41.0 | −32.6 | −58.2 | −16.1 |
| 20 | $C_{2v}$ | −37.6 | −29.3 | −57.0 | −15.5 |
| 20 | $C_1$ | −40.4 | −31.4 | −57.7 | −15.8 |
| 20 | $C_1$ | −38.3 | −28.5 | −55.7 | −13.6 |
| $As_{18+10n}$ $C_{2v}$, Figure 1 | | | | | |
| 18 | $C_{2v}$ | −42.6 | −34.5 | −60.1 | −18.7 |
| 28 | $C_{2v}$ | −48.7 | −39.6 | −72.1 | −26.3 |
| 38 | $C_{2v}$ | −51.6 | −42.0 | −77.3 | −29.6 |
| 58 | $C_{2v}$ | −54.3 | −44.2 | −82.8 | −32.8 |
| 78 | $C_{2v}$ | −55.7 | −45.4 | −85.4 | −34.4 |
| 118 | $C_{2v}$ | −57.0 | −46.4 | – | – |
| 148 | $C_{2v}$ | −57.5 | −46.9 | – | – |
| ring-shaped $As_{10n}$, Figure 1 | | | | | |
| 80 | $D_{4d}$ | −48.1 | −33.6 | −80.5 | −28.0 |
| 120 | $D_{12h}$ | −58.5 | −46.5 | −92.2 | −38.9 |
| | | | | (−110.0) | |
| 150 | $D_{15h}$ | −59.5 | −48.2 | – | – |
| $As_{18+12n}$, Figure 2 | | | | | |
| 30 | $C_2$ | −50.9 | −41.4 | −75.0 | −28.5 |
| 42 | $C_s$ | −54.3 | −44.3 | −81.3 | −32.7 |
| 42 | $C_2$ | −54.3 | −44.3 | −81.4 | −32.6 |
| 66 | $C_s$ | −57.4 | −46.9 | −87.0 | −36.4 |
| 66 | $C_2$ | −57.5 | −47.0 | −87.1 | −36.4 |
| 78 | $C_2$ | −58.3 | −47.6 | −88.5 | −37.3 |
| 90 | $C_2$ | −59.0 | −48.2 | −89.8 | – |
| 114 | $C_s$ | −59.7 | −48.8 | −91.4[b] | – |
| ∞[b] | – | −63.0 | −51.6 | −97.2 | – |
| ring-shaped $As_{24n}$ $D_{nd}$, Figure 2 | | | | | |
| 96 | $D_{4d}$ | −59.5 | −47.2 | −92.7 | −39.4 |
| 120 | $D_{5d}$ | −62.7 | −51.0 | −96.3 | −42.7 |
| 144 | $D_{6d}$ | −62.7 | −51.3 | −96.0 | – |
| icosahedral clusters, Figure 3 | | | | | |
| 20 | $I_h$ | −7.8 | −0.1 | −7.8 | 37.3 |
| 80 | $I_h$ | −34.0 | −15.2 | −72.5 | −19.4 |

[a] MP2 value. [b] Extrapolated value for the series $As_{18+12n}$ according to Equation (2).

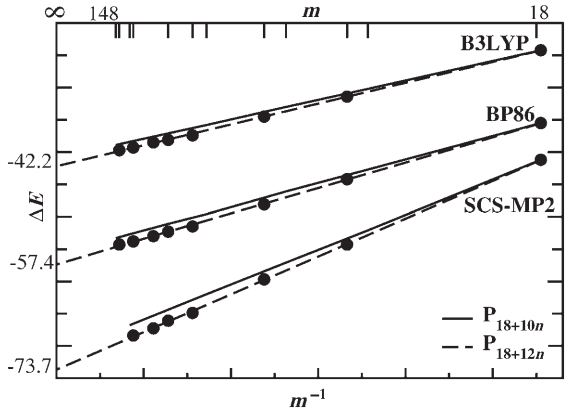


Figure 5. Fit of reaction energies $\Delta E$ in kJ mol$^{-1}$ ($P_4$) for two families of clusters $P_m$ from Table 1, as explained in text. Lines obtained from the regression [Eq. (2)], full circles represent computed $\Delta E$ data for $P_{18+12n}$.

cedures, either by measurements or by accurate CCSD(T) results, is lacking, we must conclude that neither of the

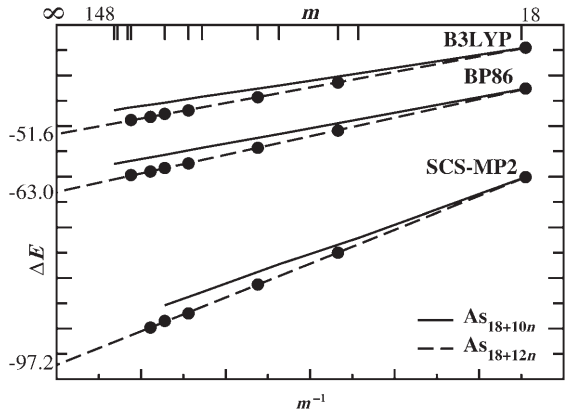


Figure 6. Fit of reaction energies $\Delta E$ in kJ mol$^{-1}$ ($As_4$) for two families of clusters $As_m$ from Table 2, as explained in text. Lines obtained from the regression [Eq. (2)], full circles represent computed $\Delta E$ data for $As_{18+12n}$.

methods available to treat systems of this size can predict $\Delta E$ with the desired accuracy of 1 kJ mol$^{-1}$ ($X_4$). Matters are not quite that hopeless, however, since differences of $\Delta E$ are quite similar for clusters of similar size: all procedures predict virtually the same ordering of $\Delta E$ (Figures 5 and 6).

To conclude this subsection, we comment briefly on basis set effects. The small SVP basis, results not documented, consistently overestimates the stability of larger clusters relative to $X_4$ by 10 to 20 kJ mol$^{-1}$ ($X_4$) in DFT treatments. This is certainly due to basis set superposition effects. The consequences of using an SVP basis can be quite dramatic: Karttunen et al. find $P_{80}$ ($I_h$) to be more stable than $P_4$ ($T_d$) by 6.7 kJ mol$^{-1}$ ($P_4$) with B3LYP, the TZVPP basis predicts $P_{80}$ to be unstable by 17 kJ mol$^{-1}$ ($P_4$) (Table 1).[2] The shortcomings of SVP-type basis sets have already been pointed out by Häser et al.[4] For the small systems $X_4$, $X_{18}$, $X_{28}$, $X_{30}$, and $X_{38}$ we have carried out SCS-MP2 calculations (at the B3LYP/TZVPP geometries) with the QZVPP basis.[37] The results are collected in Table 3. A comparison with results in

Table 3. Computed SCS-MP2 reaction energies $\Delta E$ in kJ mol$^{-1}$ ($X_4$, X = P, As) obtained with the QZVPP basis set, nomenclature as in Tables 1 and 2.

| $m$ | G | P | As |
|---|---|---|---|
| 4 | $T_d$ | 0.0 | 0.0 |
| 18 | $C_{2v}$ | −45.5 | −54.8 |
| 28 | $C_{2v}$ | −56.9 | −66.0 |
| 30 | $C_2$ | −59.1 | −68.8 |
| 38 | $C_{2v}$ | −62.0 | −70.9 |

Table 1 and Table 2 shows that TZVPP underestimates the stability of $P_m$ by roughly 4.6 kJ mol$^{-1}$ ($P_4$) and overestimates the one of $As_m$ by roughly 5.8 kJ mol$^{-1}$ ($As_4$). The deviation depends on system size $m$, which would allow us to extrapolate QZVPP results for the remaining clusters. A decompo-

[2] We have checked the correctness of the B3LYP results given in reference [19] by employing the basis set used in that work.

  

sition of the total SCS-MP2 energy into an SCF and a correlation contribution shows that the latter amounts to about 80% of the deviation between TZVPP and QZVPP.

**Computed reaction energies $\Delta E$:** The computed reaction energies collected in Tables 1 and 2 and shown in Figures 5 and 6, are easily interpreted since BP86, B3LYP, and SCS-MP2 predict the same energetic order for clusters of comparable size, and $P_m$ and $As_m$ show very similar trends. The remarkable consistency of computed $\Delta E$ within the series $X_{18+10n}$ and $X_{18+12n}$ is also reflected by the quality of a regression analysis for the ansatz (2),

$$\Delta E(X_m) = a + \frac{b}{m} \quad (2)$$

which leads to an rms of less than 0.2 kJ mol$^{-1}$ ($X_4$). This permits an extrapolation of $\Delta E$ for larger clusters, as done in Tables 1 and 2.

Among the open structures, $X_{18+12n}$ is definitely more stable than the curved isomers $X_{18+10n}$ with $C_{2v}$ symmetry. A direct comparison is possible for $P_{78}$: the SCS-MP2 energy of the $C_2$ structure is 33 kJ mol$^{-1}$ lower than that for the $C_{2v}$ structure. For $As_{78}$ the difference is even 60 kJ mol$^{-1}$. The $X_{18+12n}$ structures are even more stable than the ring-shaped $X_{10n}$ structures. The isomers of $X_{18+12n}$ are virtually isoenergetic, as conjectured in the Computational Procedures section: values of $\Delta E$ [Eq. (1)] differ by 0.1 kJ mol$^{-1}$ ($X_4$) at most, as documented in Tables 1 and 2 for $X_{66}$ with $C_s$ and $C_2$ symmetry. The helical structures are slightly favored energetically for all methods in all cases investigated.

The smallest $\Delta E$ values are obtained for the ring-shaped $X_{24n}$ systems ($D_{nd}$), which assume a minimum for $P_{144}$ and $As_{120}$. The smaller and larger structures of this type are strained, as we checked for P: structure parameters of $P_{66}$ ($C_s$) (Figure 2) show virtually perfect angles necessary for a ring closure. The computed $\Delta E$ value for the most stable rings is thus expected to be close to that of an infinite chain $(X_2X_{10})_\infty$. This is confirmed by the results (Tables 1 and 2): extrapolated $\Delta E$ values for the chains deviate by 0.9 kJ mol$^{-1}$ ($X_4$) at most from those of the most stable rings.

The icosahedral clusters $P_{20}$ and $P_{80}$ are computed to be considerably less stable than other structures of similar size for all computational methods applied in this work. $P_{80}$ ($I_h$) is not even stable with respect to 20 $P_4$ ($T_d$) within B3LYP. The situation is similar for $As_{20}$ and $As_{80}$, although the energy differences with respect to other clusters is considerably smaller than for phosphorus. The known icosahedral cluster ion $[(AsNi_{12})As_{20}]^{3-}$ shows, however, that cages may be stabilized to yield very interesting compounds.[24]

Finally, the family of isomers $X_{18+12n}$ is outstanding in various respects: with the exception of ring-shaped $X_{24n}$ structures $As_{96}$, $X_{120}$, $X_{144}$, and $X_{168}$, it is the lowest in energy, it has a large statistical weight of $2^{n-1}$, and it permits the construction for large $n$, which is not possible without strain for the curved $C_{2v}$ structures $X_{18+10n}$.

**Low-energy structures of $P_{20}$ and $As_{20}$:** Häser et al.[4] have mentioned three low-energy structures for $P_{20}$ with $C_{2h}$, $C_{2v}$, and $C_1$ symmetry. The energetic order is not conclusive since only very small basis sets have been used. The genetic algorithm finds the $C_{2h}$ and the $C_{2v}$ structures only after 300 generations. It locates two low-lying $C_1$ structures (Figure 4). The first $C_1$ structure complies with the description $P_{10}P_2P_8$ of Häser et al. For $P_{20}$, the $C_{2v}$ isomer is only slightly favored over the $C_{2h}$ isomer for SCS-MP2, both DFT functionals give the reverse ordering. The $C_1$ structure is 15.6 kJ mol$^{-1}$ higher in energy (corresponding to $\Delta E = 3.1$ kJ mol$^{-1}$ ($P_4$), Table 1), the $C_1$ isomer is even higher, 30 kJ mol$^{-1}$ above the $C_{2v}$ structure.

Matters are only slightly different for $As_{20}$. The $C_{2h}$ isomer is most stable for all procedures, followed by the $C_1$ structure, which is just 2.2 kJ mol$^{-1}$ higher (SCS-MP2). Even the $C_{2v}$ and $C_1$ isomers are only marginally less stable (5.8 and 12.6 kJ mol$^{-1}$, SCS-MP2). All four isomers of $As_{20}$ are thermodynamically stable with respect to $As_4$, quite different from $P_{20}$.

**Effects of vibration and temperature**: Thermodynamic equilibrium depends (in addition to electronic energies) on vibrational, rotational, and translational degrees of freedom and their temperature dependence. These effects are easily evaluated if one assumes ideal gas behavior and validity of the harmonic approximation for vibrations, provided harmonic frequencies are known. We have computed the latter within BP86/SVP, with the exception of largest clusters, and evaluated the contribution $\Delta F$ to the Helmholtz free energy at ambient conditions. The SCS-MP2 + $\Delta F$ entries in Tables 1 and 2 include $\Delta F$ in addition to SCS-MP2 results of Equation (1). The small molecules $P_4$ and $As_4$ are clearly favored by $\Delta F$, but for the larger clusters we find a very smooth behavior of $\Delta F$. The variation of this quantity is certainly smaller than the probable error of computed energies. For this reason we refrain from a detailed discussion and only note the most important effect. The gain in energy seen for the larger clusters is almost compensated by $\Delta F$ such that the resulting corrected values show much smaller variations and indicate reduced thermodynamic stability than inferred from the electronic term.

## Conclusions

We have investigated two families of one-dimensional polymers of phosphorus and arsenic: $X_{18+10n}$ with $C_{2v}$ symmetry and $X_{18+12n}$, where the latter constitutes a set of $2^{n-1}$ isomers of almost identical energy. The series $X_{18+12n}$ is definitely more stable than the series $X_{18+10n}$, thus confirming a conjecture of Häser.[4] From the chains one can further form ring-shaped structures by deleting $X_8$ end groups and ring closure, leading to $X_{10n}$ with $D_{nh}$[19] and $X_{24n}$ with $D_{nd}$ symmetry. The rings are more stable than the corresponding chains in the (approximate) range $X_{120}$ to $X_{200}$.[19,20] The $X_{10n}$ structures are less stable than the $X_{18+12n}$ chains; the most

  

stable compounds found are the $D_{nd}$ structures $As_{96}$, $X_{120}$, $X_{144}$, and $X_{168}$ (and possibly $X_{192}$, which was not investigated). All these clusters are markedly more stable than the icosahedral structures of $X_{20}$ and $X_{80}$.

The present results are generally in agreement with those of Karttunen et al.[19,20] as far as comparison is possible. Deviations result from differences in basis sets (more extended in this work) and methods employed (MP2 vs. SCS-MP2).

The clusters mentioned so far were essentially obtained from motifs first discussed by Häser et al.[4,10] A rigorous search for low-energy isomers of $X_{20}$ turned out to be of little help, since the genetic algorithm required 300 generations to find the known isomers with $C_{2v}$ and $C_{2h}$ symmetry. Two low-energy structures with $C_1$ symmetry were located that are close in energy to the most stable $C_{2h}$ or $C_{2v}$. There is an urgent need for procedures to locate low-energy isomers, which are more efficient than either a molecular dynamics run with simulated annealing or a genetic algorithm.

Effects of vibrations and temperature favor the small $T_d$ tetramers $X_4$, the corresponding contributions $\Delta F$ cancel to a large extent the gain in electronic energy seen for the larger clusters.

Clusters of phosphorus and arsenic have many features in common, reflecting their close chemical similarity, which has been rationalized by Pyykkö[28] in terms of partial 3d-screening. Besides the small tetrahedral compounds $X_4$, there is a rich zoo of local minima, but the energetically and thermodynamically most stable structures are low-symmetry chains of the family $X_{18+12n}$, which are surpassed in stability only by rings $X_{24n}$. Both types of clusters do not lead to space-filling solids, but they should be detectable under suitable conditions.

## Acknowledgements

We thank David Tew for critically reading the manuscript. This work was supported by the "Deutsche Forschungsgemeinschaft" (Research Center for Functional Nanostructures) and the "Fonds der Chemischen Industrie". We thank the unknown referees for their suggestions and for indicating useful references.

[1] R. Ahlrichs, M. Bär, H. Horn, C. Kölmel, *Chem. Phys. Lett.* **1989**, *162*, 165–169.
[2] A. D. Becke, *Phys. Rev. A* **1988**, *38*, 3098–3100.
[3] A. D. Becke, *J. Chem. Phys.* **1993**, *98*, 5648–5652.
[4] S. Böcker, M. Häser, *Z. Anorg. Allg. Chem.* **1995**, *621*, 58–286.
[5] S. Brode, H. Horn, M. Ehrig, D. Moldrup, J. E. Riee, R. Ahlrichs, *J. Comput. Chem.* **1993**, *14*, 1142–1148.
[6] P. D. Dacre, *Chem. Phys. Lett.* **1970**, *8*, 625–627.
[7] S. Grimme, *J. Chem. Phys.* **2003**, *118*, 9095–9102.
[8] S. Grimme, *J. Chem. Phys.* **2006**, *127*, 187–1799.
[9] J. G. Hanand, J. Morales, *Chem. Phys. Lett.* **2004**, *396*, 27–33.
[10] M. Häser, *J. Am. Chem. Soc.* **1994**, *116*, 6925–6926.
[11] M. Häser, R. Ahlrichs, *J. Comput. Chem.* **1989**, *10*, 104–111.
[12] M. Häser, U. Schneidr, R. Ahlrichs, *J. Am. Chem. Soc.* **1992**, *114*, 9551–9568.
[13] M. Häser, O. Treutler, *J. Chem. Phys.* **1995**, *102*, 3703–3711.
[14] C. Hättig, *Phys. Chem. Chem. Phys.* **2005**, *7*, 59–66.
[15] C. Hättig, A. Helweg, A. Köhn, *Phys. Chem. Chem. Phys.* **2006**, *8*, 1159–1169.
[16] J. G. Hill, J. A. Platts, H. J. Werner, *Phys. Chem. Chem. Phys.* **2006**, *8*, 4072–4078.
[17] W. Hiller, K.-W. Klinkhammer, W. Uhl, J. Wagner, *Angew. Chem.* **1991**, *103*, 182–183; *Angew. Chem. Int. Ed. Engl.* **1991**, *30*, 179–180.
[18] P. Jurečka, J. Šponer, J. Černý, P. Hobza, *Phys. Chem. Chem. Phys.* **2006**, *8*, 1985–1993.
[19] A. J. Karttunen, M. Linnolahti, T. A. Pakkanen, *Chem. Eur. J.* **2007**, *13*, 5232–5237.
[20] A. J. Karttunen, M. Linnolahti, T. A. Pakkanen, *ChemPhysChem* **2007**, *8*, 2373–2378.
[21] H. W. Kroto, J. R. Heath, S. C. O'Brien, R. F. Curl, R. E. Smalley, *Nature* **1985**, *318*, 162–163.
[22] C. Lee, W. Yang, R. G. Par, *Phys. Rev. B* **1988**, *37*, 785–789.
[23] X. Li, K. Boggavarapu, J. Li, H. J. Zhai, L. S. Wang, *Angew. Chem.* **2002**, *114*, 4980–4983; *Angew. Chem. Int. Ed.* **2002**, *41*, 4786–4789.
[24] M. J. Moses, J. C. Fettinger, B. W. Eichorn, *Science* **2003**, *300*, 778–780.
[25] J. Perdew, *Phys. Rev. B* **1986**, *33*, 8822–8824.
[26] J. Perdew, *Phys. Rev. B* **1986**, *34*, 7406.
[27] A. Pfitzner, E. Freudenthaler, *Angew. Chem.* **1995**, *107*, 1784–1786; *Angew. Chem. Int. Ed. Engl.* **1995**, *34*, 1647–1649.
[28] P. Pyykkö, *J. Chem. Res. S* **1979**, 380–381.
[29] P. Pyykkö, N. Runebrg, *Angew. Chem.* **2002**, *114*, 2278–2280; *Angew. Chem. Int. Ed.* **2002**, *41*, 2174–2176.
[30] C. C. J. Roothaan, *Rev. Mod. Phys.* **1951**, *23*, 69–89.
[31] M. Sierka, J. Dobler, J. Sauer, G. Santambrogio, M. Brummer, L. Wöste, E. Janssens, G. Meijer, K. R. Asmis, *Angew. Chem.* **2007**, *119*, 3437–3440; *Angew. Chem. Int. Ed.* **2007**, *46*, 3372–3375.
[32] J. C. Slater, *Phys. Rev.* **1951**, *81*, 385–390.
[33] M. von Arnim, R. Ahlrichs, *J. Comput. Chem.* **1998**, *19*, 1746–1757.
[34] M. von Arnim, R. Ahlrichs, *Can. J. Phys.* **1999**, *1*, 9125–9445.
[35] S. Vosko, L. Wilk, M. Nussair, *Can. J. Phys.* **1980**, *58*, 1200.
[36] F. Weigend, *Phys. Chem. Chem. Phys.* **2006**, *8*, 1057–1065.
[37] F. Weigend, R. Ahlrichs, *Phys. Chem. Chem. Phys.* **2005**, *7*, 3297–3305.
[38] Q. Wu, W. Wang, *J. Chem. Phys.* **2002**, *116*, 515–524.
[39] J. A. Wunderlich, W. N. Lipscomb, *J. Am. Chem. Soc.* **1960**, *82*, 4427–4428.

Received: December 6, 2007
Published online: March 26, 2008

  